Published version at https://link.springer.com/article/10.1007/s11104-019-04061-6

Sánchez-Sánchez, A., Cerdán, M., Jordá, J.D. et al. Plant Soil (2019) 439: 447.

https://doi.org/10.1007/s11104-019-04061-6

Characterization of soil mineralogy by FTIR: Application to the analysis of mineralogical changes in soils affected by vegetation patches.

A. Sánchez-Sánchez a, M. Cerdán a, J.D. Jordá b,∗, B. Amat c, J. Cortina b,c,

a Dep. Agrochemistry and Biochemistry, Faculty of Sciences, University of Alicante, Ap. 99, 03080 Alicante, Spain. dab@ua.es

b Institute for Environmental Research, Ramon Margalef, University of Alicante, Ap. 99, 03080 Alicante, Spain. imem@ua.es,

c Department of Ecology, Faculty of Sciences, University of Alicante, Ap. 99, 03080 Alicante, Spain. deco@ua.es

*corresponding author : juana.jorda@ua.es, Phone/Fax +34 96 590 9873

Abstract

Aims

The objective of this paper was to develop a method based on infrared spectroscopy to compare mineral content in soils and apply it to evaluate soil mineralogical variations in pairs of inter-patch and patch soils in a semi-arid area.

Methods

Mixtures of several minerals were analyzed by infrared spectroscopy, the second derivative of the spectra was calculated and the spectra normalized respect to calcite or quartz signals (711cm^{-1} or 800 cm^{-1} respectively). The intensities of representative signals of each mineral were related to their concentration in the mixtures. Pairs of patch and inter-patch soils from five different sites were analyzed by this method. Elemental analysis and total lime analysis were performed in some soil pairs.

Results

Soils were dominated by calcite and quartz, or by montmorillonite and kaolinite. Inter-patch soils were richer in calcite and poorer in quartz or clays than patch soils. Calcite losses in patch soils might be related to soil acidification by CO_2 from respiration and/or organic matter. Elemental analysis showed high values of S, Cl, and K in patch soils with respect to inter-patch soils.

Conclusions

The proposed FTIR method was useful to compare soil mineralogy in specific areas. Fertile spots by accumulation of water, soluble salts and sediments may favor plant growth in semi-arid regions and these plants may increase the fertility of the spot. Changes in soil mineral composition could be used to monitor the biological activity of soil in arid and semi-arid zones

Keywords:, FTIR, XRF, quartz, clays, calcite, dolomite

Introduction

In areas with water or nutrient limitations, patches of vegetation produced by plant interactions are observed. Unpopulated or sparsely populated vegetation areas alternate with areas of dense vegetation of trees or shrubs (Lejeune et al. 2002).

Vegetation patches are considered fertility islands attracting other species in arid and semi-arid areas. Vegetation is able to secrete substances that help solubilizing mineral nutrients, contributing significantly to weathering. For instance, it is known that phenols are involved in the mobilization of nutrients such iron (Fe) and phosphorus (P) by plants (Marschner 1995). The scarcity of nutrients in soil involves competition for these nutrients and finally, determines the composition of plant communities. The substances excreted by plants roots, for mineral weathering and nutrient uptake, facilitate the growth of other species nearby (Raynaud et al. 2008). Soil microorganisms also play an important role in mineral weathering, and microorganisms are abundant in plant rhizosphere (Bakker et al. 2013). Banfield et al. (1999) found significant dissolution of biotite and feldspar, using cultures of microorganisms and polysaccharides. According to Motamedi et al. (2013) vegetation patches in saline rangelands have higher amounts of total soil P, less acidity, electrical conductivity and soluble salts than the areas between patches, whereas no difference in the N content and silt was found in the 0-15 cm soil layer or the subsoil layer (15-30 cm).

The development of new spectroscopic techniques for the analysis of solids, such as Fourier transform infrared spectroscopy (FTIR) facilitates studying soil mineralogy, (Jordá et al., 2015). FTIR has been used mainly for mineral identification, because of the characteristic absorption bands in the middle infrared (IR) (400 and 4000 cm^{-1}). The technique has been used successfully in studies of mineral mixtures (Matteson and Herron 1993; Xu et al. 2001) and soil components (Yin et al. 2012; Calderon et al. 2013; Towett et al. 2015). However, signal overlapping or effects of particle size on

FTIR absorbance signals make it difficult to make quantitative analysis by this method, although semi-quantitative approaches in combination with other techniques are possible (Jordá et al. 2014; Craddock et al. 2017).

The objective of this paper was to develop a tool able to quantify the impact of vegetation patches on the rock weathering and/or sediment accumulation, with a minimum soil alteration. To do that, we have developed a method based on FTIR and applied it to compare soil samples that differed only in the plant community growing on them. We studied the possible variations in the mineralogy of 52 patches of vegetation compared to the inter-patch soil in a semiarid region of southeastern Spain.

Materials and Methods

FTIR signal evolution with mineral concentration, development of a method for soil mineralogy study

ATR-FTIR spectra of pure mineral samples were obtained (between 600 and 4000 cm^{-1} , with a wavenumber interval of 2 cm^{-1} and 64 scans), in order to serve as reference for soil spectra analysis. The ATR is a sampling mode in which the IR beam is projected in a crystalline surface of high refractive index. It is a versatile method that minimizes sample preparation. The number of mineral samples was 104 and included quartz and other silicon oxides (silex, opal, chalcedony and amorphous SiO_2); K-feldspars, plagioclases, and 1:1 and 2:1 clay minerals among others. Lignin, cellulose, pectin, starch (Sigma®) and several samples of anthracite, black amber and coal were also analyzed by FTIR, as standards for organic matter. In addition, mixtures with different combinations of the minerals present in Alicante province were also analyzed by ATR-FTIR. In mixtures, we need a reference signal to compare the intensities of the rest of the signals with it. Calcite, quartz and illite signals were analyzed as a reference. These

93 are the most abundant minerals in Alicante province and they all show definite
94 absorbance signals in FTIR. The second derivative of the spectra usually provides
95 clearer signals, and then it was also calculated for all minerals and mixtures. The linear
96 relationship between the concentration of minerals in a mixture, and their FTIR signal
97 intensity relative to the reference mineral, was explored by regression analyses
98 (Microsoft , Excel®).

99 *Impact of vegetation patches on soil mineralogy*

100 Fifty two pairs of soils in vegetation patches and in inter-patch areas were sampled (104
101 soil samples in total). Soils were taken from 5 different locations named from south to
102 north: Orihuela, Tibi, Campello, Busot and Aigües (Alicante, Spain), an area under
103 severe desertification risk (Amat, 2015). The 5 locations were chosen in order to scan,
104 from south to north, the dry zone of the province of Alicante. The main climatic,
105 situation and soil and vegetation characteristics, are summarized in Table 1.
106 Calciorthids and Torriorthents (Soil Taxonomy) alternate in all sampled areas. From a
107 geological point of view, Orihuela soils have been developed on a Neogene basin in
108 which sediments of continental origin are deposited, while Tibi, Campello, Busot and
109 Aigües soils were developed on ancient marine sediments of the middle-lower Miocene
110 (Tibi) or Jurassic, Cretaceous and Paleogene (Campello, Busot, Aigües) (De Ruig 1992,
111 Estévez et al., 2004). Annual rainfall ranges between 200 and 400 mm. These
112 environmental conditions result in alpha grass steppes (*Stipa tenacissima* L.) with
113 woody vegetation patches. Most of the patches are plurispecific with *Quercus coccifera*,
114 *Pistacia lentiscus* and *Rhamnus lycioides* as dominant species, and to a lesser extent
115 *Juniperus oxycedrus* and *Ephedra* (Amat 2015). The species with the largest canopy
116 area was considered the dominant species (Table 1).

117 The inter-patch soil was sampled at a distance of at least 2 m from the outer edge of
118 each patch, to minimize any influence of the vegetation patch. The top 5 cm of soil were
119 sampled with a probe. At least 4 sub-samples within each patch were collected and
120 mixed in a plastic bag that was carried to the laboratory. The soil samples were air-
121 dryed for 24 h, ground with a mortar and analyzed by FTIR, between 600 and 4000 cm^{-1}
122 , with a wavenumber interval of 2 cm^{-1} and 64 scans.

123 The identification of the minerals contained in each soil, was made by comparing the
124 FTIR spectra of the soils with the FTIR spectra of mineral samples. Second derivative
125 of the spectra was also calculated in order to improve the identification. To compare soil
126 composition in patches and in inter-patch areas, the FTIR signals of specific minerals
127 were used; calcite was the reference mineral for all soils, except for Orihuela where, due
128 to the low concentration of calcite, quartz was used as a reference. To do so, FTIR
129 spectra were normalized to the 711 cm^{-1} signal of the 2^{nd} derivative (calcite signal), and
130 Orihuela soils to the 781 cm^{-1} signal (quartz signal) in agreement with the results
131 obtained in the previous subsection. In addition, two pairs of patch and inter-patch soils
132 of each location were analyzed by XRF (PHILIPS MAGIX PRO, with Rh tube and Be
133 window), and the elemental composition was compared. Total lime was also measured
134 in these soils by volumetric calcimetry.
135 Pairwise statistical analyses were made with the Excel software (Microsoft®). The
136 pairwise statistical method is based on the t-student test and designed to compare data in
137 2 numeric columns to test if the differential factor between the columns affects the data
138 (Salkind, 2010). In this paper, we analyze soil under vegetation patches (column1) and
139 the same soil in an inter-patch area (column 2). Each couple patch and inter-patch soil
140 shares the same location, slope, rain, etc. and the difference is the type of vegetation that
141 grows in each soil.

142

143 **Results**

144 *Development of a method based on FTIR to compare mineralogy of soils, signal*
145 *evolution in mineral mixtures*

146 According to the FTIR results for soils (next subsection), it was investigated the
147 changes in signal intensity in mixtures of different minerals, using calcite or quartz as a
148 reference. One of the main problems with FTIR analysis is that many signals overlap,
149 and they cannot be assigned to a pure component. This causes difficulties both in
150 identification and concentration calculation. The use of the second derivative helps in
151 signal identification and interpretation and both calcite and quartz spectra show strong
152 and well-defined FTIR signals in the interval 600-1200 cm^{-1} which are very useful in
153 the identification of minerals in mixtures and can be used as a reference. For example,
154 sodium carbonate and calcite are easily distinguished because the former has a double
155 signal at 693-700 cm^{-1} and an intense signal at 876 cm^{-1} , while the latter shows signals
156 at 711, 845 and 871 cm^{-1} (Fig 1). However, a mixture of both carbonates (50% mol)
157 shows a FTIR spectrum almost identical to pure $CaCO_3$ (Fig. 1) because of their
158 different molar absorptivities. The FTIR signals produced by a mol of calcite are much
159 more intense than those produced by a mol of sodium carbonate and this is one of the
160 main problems when measuring mineral concentrations in a sample.

161 Similar results were obtained for mixtures of calcite-aragonite or calcite-dolomite
162 (under 20% dolomite mol). However, we do see some variations in the spectra that can
163 be used to compare samples with the same components but with different
164 concentrations. In all these mixtures, the calcite characteristic signals at 711 and 871
165 cm^{-1} decrease. For instance, the intensity at 711cm^{-1} (second derivative) for pure calcite

166 is -0.046 and in the mixture with sodium carbonate -0.037 (Fig 1). That may be used to
167 compare samples of similar characteristics.

168 *Development of a method based on FTIR to compare mineralogy of soils, reference*
169 *signal selection*

170 The 711 and 871 signals are well defined for calcite in the 2nd derivative spectrum and
171 might be used as a reference. However, the signal at 871 cm^{-1} is altered in the presence
172 of clays, Ca oxide and other carbonates, which absorb IR radiation at this wavenumber.
173 Aragonite shows a double signal at 700 and 711 cm^{-1} , but it practically disappears even
174 in mixtures of aragonite/calcite 1:1 (data not shown). CaO or $Ca(OH)_2$ cannot be ruled
175 out in soils as calcareous as those in this study. Their FTIR spectra also show signals at
176 712 cm^{-1}, but with a lower intensity than calcite. The 711cm^{-1} signal was then used as a
177 reference, and the spectra intensities were re-calculated on this basis; i.e. calcite pure
178 spectrum was divided by 0.046 and the spectrum of the mixture Na_2CO_3:$CaCO_3$ (1:1)
179 by 0.037, according to the results of the previous subsection. In this way the value of the
180 711 cm^{-1} signal in all the FTIR spectra is -1. By doing so for several mixtures
181 Na_2CO_3:$CaCO_3$, the signal at 1383 cm^{-1} increases linearly as the rate of calcite
182 decreases (Fig. 2a, c), but no variations were observed in the 2nd derivative signals of
183 calcite (Fig. 2b). No signals of Na_2CO_3 were observed at any concentration. However,
184 in this way we could establish if calcite is more or less concentrated in a mixture
185 although we do not know the nature of all the minerals present in the mixture.

186 On the contrary, for dolomite/calcite mixtures, changes in second derivative signals
187 were observed in addition to the changes in the 1383 cm^{-1} signal and were also related
188 to concentration (Fig. 3a). In mixtures of dolomite:calcite>0.2 (mol dolomite:mol
189 calcite), dolomite was easily distinguished by the 2nd derivative signal at 728 cm^{-1} (Fig.

190 3b). The intensity of the signal at 728 cm^{-1} increased with the ratio of dolomite/calcite
191 and showed two intervals of linearity. The first one was related to calcite signals and
192 was more intense than the dolomite signals, and the second one was related to dolomite
193 signals was more intense than calcite signals.

194 In the case of minerals whose signals do not overlap with those of calcite, the results are
195 similar. For example, equivalent results were obtained for the calcite-montmorillonite or
196 calcite-quartz mixtures. Quartz showed intense signals at 781 cm^{-1} , 798 cm^{-1} and 1164
197 cm^{-1} in the 2nd derivative spectrum. Clay minerals also absorb IR at 800 cm^{-1} and the
198 signal at 1164 cm^{-1} is the lowest, so the signal at 781 cm^{-1} can be taken as a reference.
199 Similar results were obtained when the signal of quartz at 781 cm^{-1} was taken as a
200 reference in mixtures of quartz and several minerals such as montmorillonite or
201 carbonates.

202 Unfortunately, changes in FTIR signals are not only owed to concentration. Other
203 factors such as particle size may take effect (Reig et al. 2002). However, when
204 comparisons are made within samples of the same location, it can be assumed that the
205 physical properties of soil mineral particles are similar, because texture is a permanent
206 quality of soils (Schaetzl and Anderson 2005), and concentration is the only effect on
207 FTIR signals. So, this method can be useful to test weathering, pollution, erosion, etc.
208 effects on a soil, by comparing unaltered soil with altered soil in the same location.

209

210 *Application of the FTIR method to the study of soil mineralogy in vegetation patches,*
211 *mineral composition of the soils*

212 The FTIR spectra were quite uniform and simple for Aigües, Busot, Campello, and Tibi
213 soils (Fig. 4). The signals at ~ 1400, 711 cm^{-1} are from carbonates or Ca oxides,

whereas the signal at ~ 1000 cm^{-1} is characteristic of clays, quartz, feldspars and other silicates, and the double signal at around 800 cm^{-1} is for quartz. No signals were obtained in the 3000-4000 cm^{-1} region. Water absorbed in clay minerals show intense signals in this region of the spectrum. That suggest that the presence of clay minerals in these soils must be low. In some spectra a small signal al 3625 cm^{-1} that could be compatible with illite, a mineral very frequent in the area, is sensed. Calcite, and quartz are then the main components of these soils. That explains its low moisture retention capacity, which together with the scarce rainfall, contributes to the semi-arid condition of the area. On the contrary, smectites and kaolinite are the main component observed in the spectra of Orihuela soils (Fig. 2). Calcite (711 cm^{-1}) and dolomite (728 cm^{-1}) are clearly distinguished in the 2nd derivative. Ca oxides show strong signals at 856 and 873 cm^{-1}. The occurrence of those later was also suggested in some soils by the displacement of the 1400 cm^{-1} absorbance signal to higher wavenumbers, but we did not observe other signals to confirm that. The presence of these clays means that the aridity condition of these soils is less severe than in the dominated by calcite and quartz, even though the annual mean rainfall is lower in this area (Table 1). We concluded that the soils are dominated by calcite in most cases, although dolomite and other carbonates could be present according to the previous subsection results. In no case were signals of organic compounds detected. The organic matter of these soils had been studied in previous research (Cerdán et al., 2015, Amat, 2015). The richest soils in organic matter (8%) corresponded to the Aigües area, and they were all at or below the detection limit of this technique (10%) (Jordá et al., 2014).

Elemental concentrations and total lime were measured in some samples to confirm the previous results (Table 2). Calcium is the major element in all soils as well as lime, except in Orihuela. Despite the aridity condition there is no special accumulation of

239 soluble salts such as gypsum or chlorides. Small concentrations of Al are detected in all
240 soils which must be related to clay occurrence. Accordingly, Orihuela soils showed the
241 highest concentration of this element in parallel with Si content. All these results are in
242 agreement with the FTIR spectroscopy data

243 *Patch and inter-patch soil comparison*

244 For Aigües, Busot, Campello and Tibi soils, the signal at 1400 cm^{-1} and the signal of
245 the silicates at 1000 cm^{-1} increased significantly in patch soils, Fig. 5a, meaning a
246 decrease in calcite in patch soils compared to inter-patch soils, i.e. inter-patch soils are
247 richer in calcite than patch soils which in turn, contain more quartz (and probably more
248 clay) than inter-patch soils. Quartz signals are quite intense in the 2nd derivative spectra,
249 Fig. 5b, and clearly increased in patch soils. This increase was mainly due to patches
250 dominated by *P. lentiscus* and *Q. coccifera*. In patches dominated by *R. lycioides*, no
251 differences were observed between patch and inter-patch soils, and in the case of *E.*
252 *fragilis* and *J. oxycedrus*, no statistically significant differences were found because of
253 the small number of patches of these species.

254 In Orihuela soils, patches were dominated by *Q. coccifera* and *P. lentiscus.* Because of
255 the lack of lime in these soils, quartz was taken as a reference. Clay minerals increased
256 significantly in patch-soils compared to quartz, Fig. 6a. No significant statistical
257 differences were observed in the 1400 cm^{-1} signal of carbonates. However, second
258 derivative signals of calcite (711 cm^{-1}) and dolomite (728 cm^{-1}) significantly
259 decreased in patch soil compared to the inter-patch areas (Fig. 6b). This means that, as
260 in the previous case, there is a decrease in the carbonate content in the patch soils
261 compared to inter-patch soils. This result is confirmed by the lime data in Table 2,
262 except for Busot soils. With respect to the clay minerals, the second derivative signals
263 in this interval are not easily attributed to a specific clay. The signals at 910 and 3619
264 cm^{-1} are for kaolinite and montmorillonite, however, signals at 1025 and 3696 cm^{-1} are
265 characteristics of kaolinite, meanwhile the signal at 1116 cm^{-1} is for montmorillonite.
266 All these clay signals are higher in patch soils than in inter-patch soils (Fig. 6b)

The elemental composition of the soils kept quite constant, but significant differences ($p<0.01$) were obtained for S, Cl and K between patch and inter-patch soils (Table 2). The soil in vegetation patches is enriched in soluble elements respect to the inter-patch soil.

Discussion

The reason for the increase of the silicate signal, particularly quartz, relative to calcite in the soils of the vegetation patches, is probably due to calcite dissolution. Calcite is an easily weatherable mineral (Schaetzl and Anderson, 2005), both by organic matter and by increased respiration due to the higher microbial biomass and root biomass in patch soils that results in high concentrations of CO_2 capable of dissolving calcite. In a previous study of the soils of this paper, we found that patch soils accumulate organic (Cerdán et al. 2016) matter. *Q. coccifera* and *P. lentiscum* produced more intense reactions than *S. tennacisima*, while *R. lycioides* has a similar effect. The patches of *R. lycioides* contained substantial amounts of organic acids (Cerdán et al., 2016), but according to the results of this work, they did not play an important role in calcite dissolution, so the hypothesis of calcite dissolution by CO_2 seems more likely. The area of the of *Q. coccifera* and *P. lentiscum* patches was much larger than that of *R. lycioides* (Amat, 2015), so their impact on the patch soil must also be higher than in *R. lycioides* patches and made them poorer in calcite and richer in quartz.

Calcite dissolution may be also the result of the different strategies used by woody species and herbaceous plants for the uptake of some nutrients such as Fe which, in some occasions, includes the acidification of the rhizosphere in the first case and the release of phytosiderophores in the second case The acidification of the rhizosphere contributes to facilitate the reduction of Fe (III) to Fe (II) which is the main mechanism

of Fe uptake in dicotyledonous plants (Marschner, 1995). These "less" calcareous patch soils may show some advantages in terms of fertility, including better water and nutrient storage and the improvement of Si uptake. Si plays a significant role in plants under water stress (Epstein, 2009) and, although this element is not limited in field condition, its dynamics in these arid environments is poorly understood. Quartz is dissolved by organic acids and complexed by citrate, oxalate and pyruvate in lab conditions similar to soil condition (pH 7 and 25ºC) (Bennett et al. 1988), and can be made use by plants in these soluble forms.

The dissolution of calcite is more evident in the soils of Orihuela, where the patches are mainly dominated by *Q. coccifera* and *P. lentiscum*. Montmorillonite is transformed into kaolinite very slowly (Schaetzl and Anderson, 2005), but it was not possible to observe a decrease in montmorillonite content related to a kaolinite increase although signals of both minerals were observed. In addition to calcite dissolution, the increase in clay content in Orihuela patch soils may be owed to clay accumulation caused by runoff and sediment transport to the patches (Reid et al., 1999; Field et al. 2012). However, it cannot be ruled out that the patch may have developed in an area of the landscape where clays had been accumulated by geological or climatic reasons, and therefore water availability could be higher in that area. This fact could also explain the highest quantities of soluble elements in patch soils and confirm the sink role of these soils. Soil moisture distribution and the abundance of xeric, mesic or hydric plants in a site depend on erosion processes (Ding et al. 2018). Water accumulation means soluble salts and suspended materials accumulation, spots of fertility in landscapes.

Conclusions

The method described in this paper for soil mineralogy comparison and based on FTIR analysis, is quick and simple to apply. The method has been tested in mineral mixtures of known composition and in field soils and the results agree with data obtained by FRX and the lime content. It would be applicable to the study of areas in which part of the soil has been altered by causes as the presence of vegetation patches, pollution, deforestation and/or mineral transformations over time. It is not necessary to calculate the exact concentration of the mineral, which on the other hand, is difficult with the current knowledge since it is necessary to estimate the extinction coefficients (Jordá et al., 2015) or the mineral elemental composition (Craddock, 2018) which can give variations above 10% in concentration estimations . In this way the experimental error is based on the error of the instrument itself and differences can be estimated in a more acute way. The method can be also useful to compare soils in different zones, but it would be necessary to assure the uniformity of the particle size, with a previous grinding, for example, similar to all soils.

Our study revealed the differences between the concentrations of minerals present in soils where patches of vegetation grow. Fertile spots by accumulation of water, soluble salts and sediments favor plant growth in semi-arid regions. In turn, vegetation transforms the soil increasing fertility, attracting new species and contributes to patch spread in those semi-arid environments. The calcite decrease in woody vegetation patches may be an indicator of intense metabolic activity. The increase in respiration and nutrient uptake due to the greater depth of the roots of the woody plants compared to the *S. tenacissima* bushes may explain, at least in part, these results. The evolution of this effect could be used to monitor the biological activity of soil in arid and semi-arid zones

339 Funding

340 Research funded by the Spanish Ministry of Science and Innovation (projects
341 UNCROACH, CGL2011-30581- C02-01 and GRACCIE Programa Consolider-Ingenio
342 2010, CSD2007-00067), Spanish Ministry of the Environment, Rural and Marine Areas
343 (Project RECUVES; 077/RN08/04.1) and Generalitat Valenciana (Programa G. Forteza;
344 FPA/2009/029).

345 *References*

346 Amat B (2015) Dynamics of woody vegetation patches in semiarid ecosystems in the
347 southeast of Iberian Peninsula. PhD Thesis. University of Alicante.
348 https://rua.ua.es/dspace/bitstream/10045/50210/1/tesis_beatriz_martinez.pdf

349 Bakker AHM, Berendsen RL, Doornbos RF, Wintermans PCA, Pieterse CMJ (2013)
350 The rhizosphere revisited: root microbiomics. Front Plant Sci. 4 165 1-7.

351 https://doi.org/10.3389/fpls.2013.00165

352 Banfield JF, Barker WW, Welch SA, Taunton, A (1999) Biological impact on mineral
353 dissolution: Application of the lichen model to understanding mineral weathering in the
354 rhizosphere. Proc Natl Acad Sci USA 96 3404–3411.

355 https://doi.org/10.1073/pnas.96.7.3404

356 Bennett BC, Melcer ME, Siegel DI, Hassett JP (1988) The dissolution of quartz in
357 dilute aqueous solutions of organic acids at 25°C. Geochim Cosmochim Acta 52 1521-
358 1530.

359 https://doi.org/10.1016/0016-7037(88)90222-0

360 Calderon F, Haddix M, Conant R, Magrini-Bair K, Paul E (2013) Diffuse-reflectance
361 Fourier-transform mid-infrared spectroscopy as a method of characterizing changes in
362 soil organic matter. Soil Science Soc Am J, 77 1591-1600.

363 https://doi.org/10.2136/sssaj2013.04.0131

364 Cerdán M, Sánchez-Sánchez A, Jordá JD, Amat B, Cortina J, Ruiz-Vicedo, N, El-
365 Khattabi M (2016) Characterization of water dissolved organic matter under woody
366 vegetation patches in semi-arid Mediterranean soils. Sci Total Environ 553 340–348.
367 https://doi.org/10.1016/j.scitotenv.2016.02.091

368 Craddock PR, Herron M, Herron SL (2017) Comparison of quantitative mineral
369 analysis by X-ray diffraction and Fourier transform infrared spectroscopy. J Sediment
370 Res, 87 630-652.

371 https://doi.org/10.2110/jsr.2017.34

372 De Ruig MJ (1992) Tectono sedimentary evolution of the prebetic fold bet of Alicante
373 (SE Spain). A study of stress fluctuations and forelan basin deformation. PhD Thesis.
374 University of Utrecht

375 Ding J, Johnson EA, Martin YE (2018) Linking Soil Moisture Variation and Abundance
376 of Plants to Geomorphic Processes: A Generalized Model for Erosion-Uplifting
377 Landscapes. J Geophys Res Biogeosci. 123 960-975.
378 https://doi.org/10.1002/2017JG004244

379 Estévez A, Vera JA, Alfaro P, Andreu JM, Tent-Manclús JE, Yébenes A (2004)
380 Alicante en la Cordillera Bética. *In Geología de Alicante*, Alfaro P, Andreu JM, Estévez
381 A, Tent-Manclús JE, Yébenes A (eds), University of Alicante, pp 39-50.

382 Epstein E (2009) Silicon: its manifold roles in plants. Ann Appl Biol 155 155–160.
383 https://doi.org/10.1111/j.1744-7348.2009.00343.x

384 Field JP, Breshears DD, Whicker JJ, Zou CB (2012) Sediment capture by vegetation
385 patches: Implications for desertification and increased resource redistribution. J
386 Geophys Res Biogeosci. 117, 1-9.

387 https://doi.org/10.1029/2011JG001663

388 Jordá JD, Jordán MM, Ibanco-Cañete R, Montero MA, Reyes-Labarta JA, Sánchez A.
389 Cerdán M (2015) Mineralogical analysis of ceramic tiles by FTIR: A quantitative
390 attempt. Appl Clay Sci. 115 1–8.

391 https://doi.org/10.1016/j.clay.2015.07.005

392 Lejeune O, Tlidi M, Couteron P (2002) Localized vegetation patches: A self-organized
393 response to resource scarcity. Phys Rev E. **66**, 1-4.
394 https://doi.org/10.1103/PhysRevE.66.010901

395 Marschner H (1995) Mineral nutrition of higher plants. Academic Press, London
396 Matteson A, Herron MM (1993) Quantitative Mineral Analysis by Fourier Transform
397 Infrared Spectroscopy. SCA Conference Paper Number 9308, pp. 1-15.
398 Motamedi J, Mirkala RM, Alizadeh A (2013) Effect of vegetation patches as micro-
399 habitats on changing the soil properties (Case study: Saline rangelands surrounding
400 Urmia Lake). Int. J. Forest Soil Erosion. **3**, 92-94

401 Raynaud X, Jaillard B, Leadley PW (2008) Plants may alter competition by modifying
402 nutrient bioavailability in rhizosphere: a modeling approach. Amer. Naturalist. 171 44–
403 58.

https://doi.org/10.1086/523951.

Reid KD, Wilcox BP, Breshears DD, MacDonald L (1999) Runoff and Erosion in a Piñon-Juniper Woodland: Influence of Vegetation Patches. Soil Sci Soc Am J. 63 1869-1879.

Reig FB, Adelantado JV, Moya-Moreno MC (2002) FTIR quantitative analysis of calcium carbonate (calcite) and silica (quartz) mixtures using the constant ratio method. Application to geological samples. Talanta. 58 811-821.

https://doi.org/10.1016/S0039-9140(02)00372-7

Salkind NJ (2010) Encyclopedia of Research Design. SAGE Publications, Inc London

http://dx.doi.org/10.4135/9781412961288

Schaetzl R, Anderson S (2005) Soils. Genesis and Geomorphology. Cambridge University Press

Towett EK, Sheperd KD, Sila A, Aynekulu E, Cadisch G (2015) Mid-infrared and total X-ray fluorescence spectroscopy complementarity for assessment of soil properties. Soil Sci Soc Am J, 79: 1375-1385

https://doi.org/10.2136/sssaj2014.11.0458

Yin K, Hong H, Li R, Han W, Wu Y, Gao W, Jia J (2012) Mineralogy and genesis of mixed-layer clay minerals in the Jiujiang net-like red soil. Spectroscopy and Spectral Analysis, 32 2765-2769.

https://doi.org/10.3964/j.issn.1000-0593(2012)10-2765-05

Xu Z, Cornilsen BC, Popko DC, Pennington, WD, Wood JR, Hwang JY (2001) Quantitative Mineral Analysis by FTIR Spectroscopy. *Internet Journal of Vibrational. Spectroscopy*, **5,** 1-4 http://www.ijvs.com/volume5/edition1/section2.html

Figure captions

Fig. 1 FTIR spectra (right) and 2nd derivative spectra (left) of Na_2CO_3, $CaCO_3$ and a mixture Na_2CO_3:$CaCO_3$ 1:1 mol:mol. Absorbance is measured in arbitrary units; abs: absorbance

Fig. 2 FTIR spectra for different Na_2CO_3/$CaCO_3$ ratios (mol:mol) (R) (a). Second derivative of the spectra (b). Linear relationship between the calcite absorbance signal at 1383 cm^{-1} and the different Na_2CO_3/$CaCO_3$ ratios. Absorbance is measured in arbitrary units; abs: absorbance

Fig. 3 Variation of the dolomite signal at 728 cm^{-1} (second derivative) with the dolomite/ calcite ratio (R), mol/mol when the calcite signal at 711 cm^{-1} is taken as a reference (a). Linear relationship between the dolomite second derivative signal at 728 cm^{-1} and the different dolomite/calcite ratios. Absorbance is measured in arbitrary units; abs: absorbance (b)

Fig. 4 FTIR spectra of the soils: a and c are the characteristic spectrum and the 2nd derivative, respectively, for a soil from Campello. Aigües, Busot, or Tibi; b and d the

447 spectrum and the 2nd derivative for Orihuela soils. Spectra are normalized to the highest
448 signal. Mt: montmorillonite; Ca:calcite; Do: dolomite; Qz: quartz; Ka: kaolinite.
449 Absorbance is measured in arbitrary units; abs: absorbance

450

451 **Fig. 5** Aigües, Busot, Campello and Tibi soils. a. Intensity of the FTIR 1000 and 1400
452 cm^{-1} absorbance signal with respect to calcite. b. Intensity of the second derivative
453 signals for quartz relative to calcite. (*): 0.05>P>0.01; (**): 0.01>P>0.001; (ns):
454 0.05<P<0.1

455

456 **Fig. 6** Orihuela soils. a. Intensity of the FTIR spectrum signals respect to quartz. b.
457 Intensity of the second derivative signals for quartz relative to quartz. (*): 0.05>P>0.01;
458 (**): 0.01>P>0.001; (ns): 0.05<P

459

460

461

462

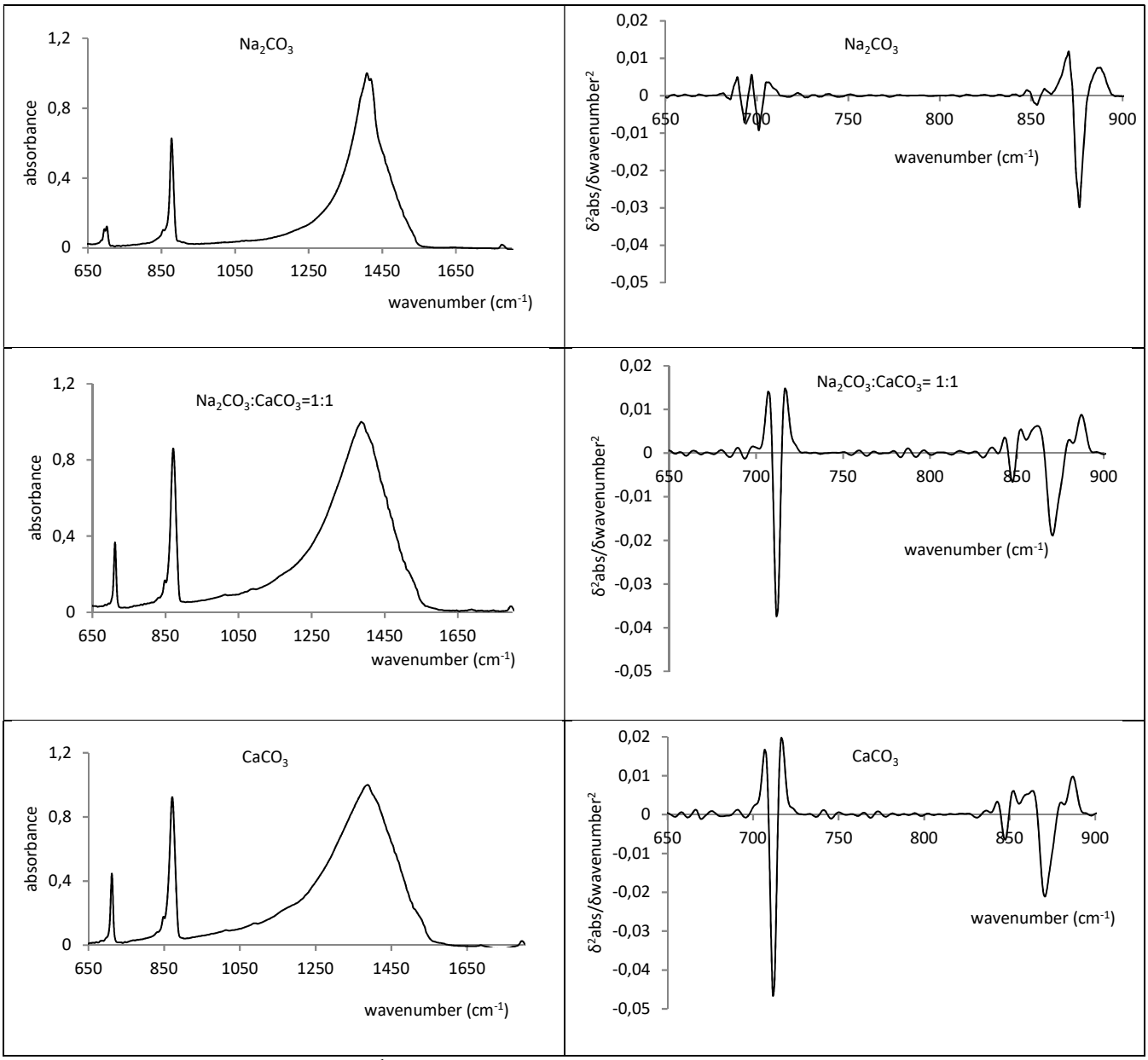

Fig. 1 FTIR spectra (right) and 2nd derivative spectra (left) of Na_2CO_3, $CaCO_3$ and a mixture Na_2CO_3:$CaCO_3$ 1:1 mol:mol. Absorbance is measured in arbitrary units; abs: absorbance

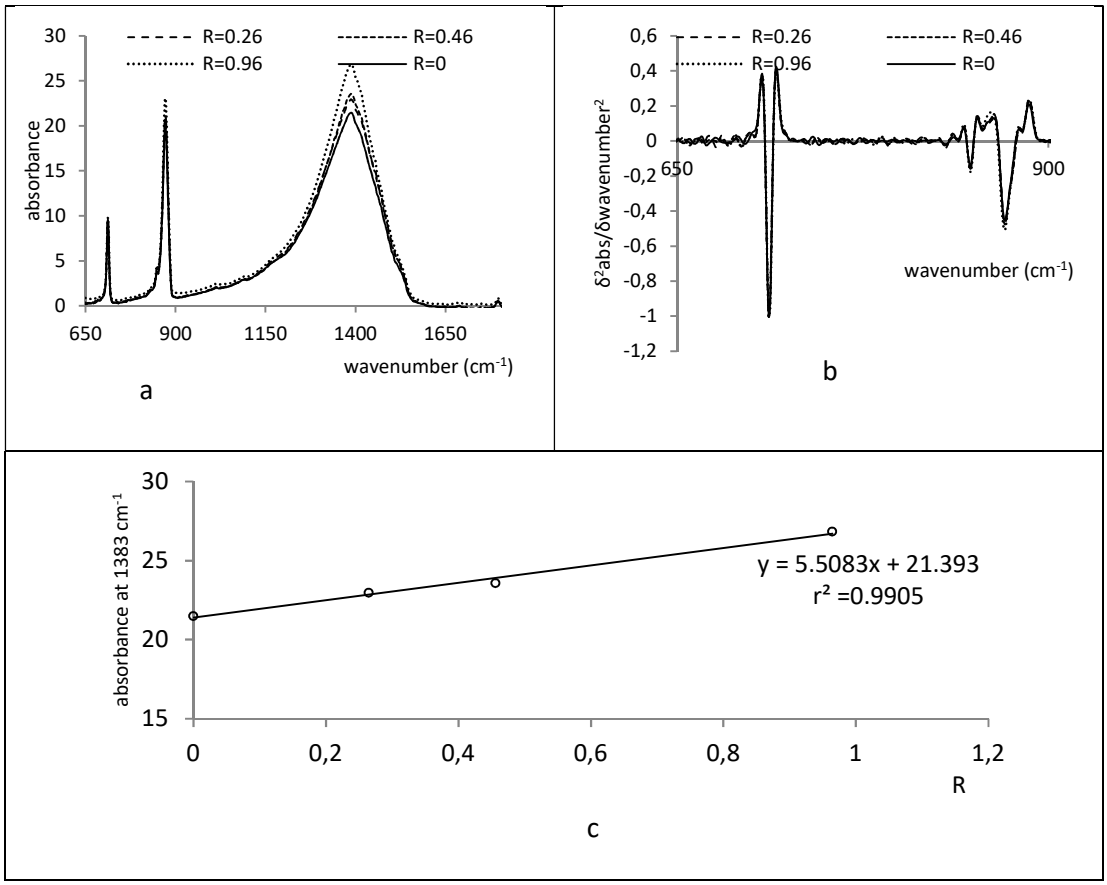

Fig. 2 FTIR spectra for different $Na_2CO_3/CaCO_3$ ratios (mol:mol) (R) (a). Second derivative of the spectra (b). Linear relationship between the calcite absorbance signal at 1383 cm^{-1} and the different $Na_2CO_3/CaCO_3$ ratios. Absorbance is measured in arbitrary units; abs: absorbance

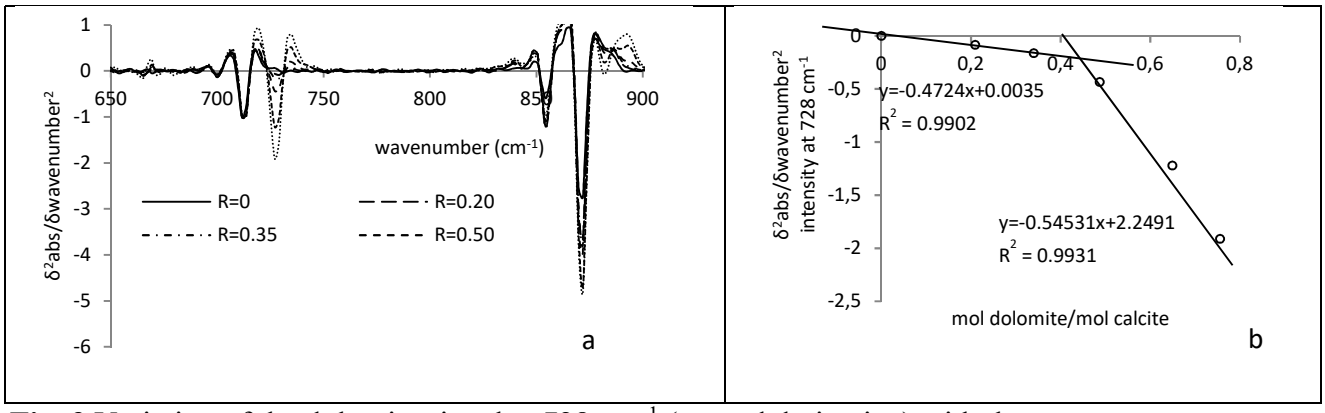

480 **Fig. 3** Variation of the dolomite signal at 728 cm^{-1} (second derivative) with the
481 dolomite/ calcite ratio (R), mol/mol when the calcite signal at 711 cm^{-1} is taken as a
482 reference (a). Linear relationship between the dolomite second derivative signal at 728
483 cm^{-1} and the different dolomite/calcite ratios. Absorbance is measured in arbitrary units;
484 abs: absorbance

485 (b)

486

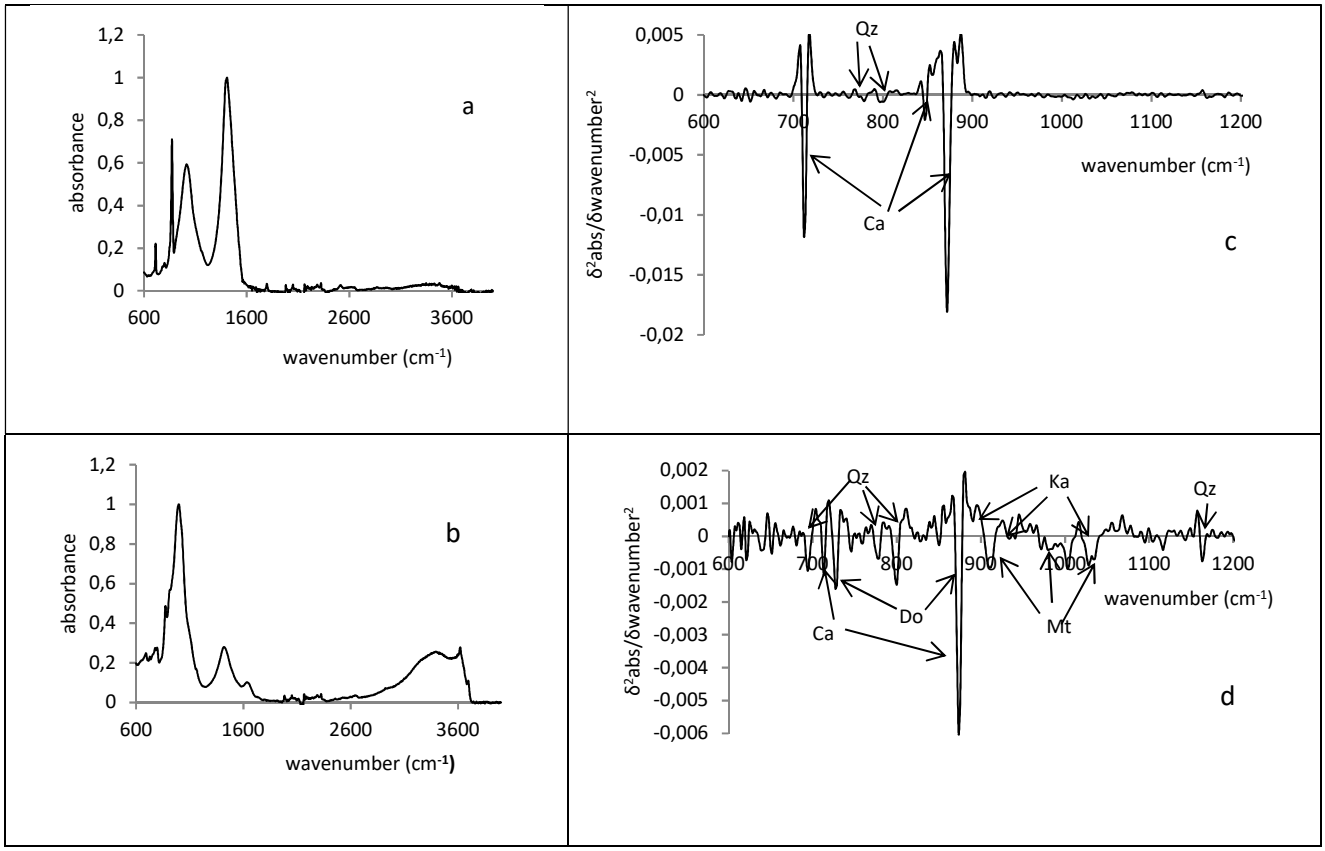

Fig. 4 FTIR spectra of the soils: a and c are the characteristic spectrum and the 2nd derivative, respectively, for a soil from Campello. Aigües, Busot, or Tibi; b and d the spectrum and the 2nd derivative for Orihuela soils. Spectra are normalized to the highest signal. Mt: montmorillonite; Ca:calcite; Do: dolomite; Qz: quartz; Ka: kaolinite. Absorbance is measured in arbitrary units; abs: absorbance

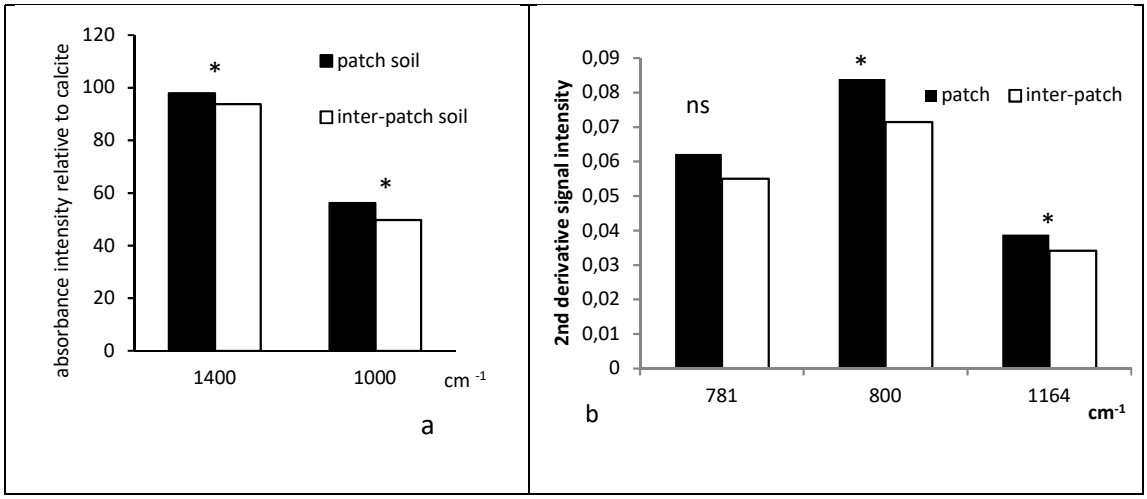

Fig. 5 Aigües, Busot, Campello and Tibi soils. a. Intensity of the FTIR 1000 and 1400 cm^{-1} absorbance signal with respect to calcite. b. Intensity of the second derivative signals for quartz relative to calcite. (*): 0.05>P>0.01; (**): 0.01>P>0.001; (ns): 0.05<P<0.1

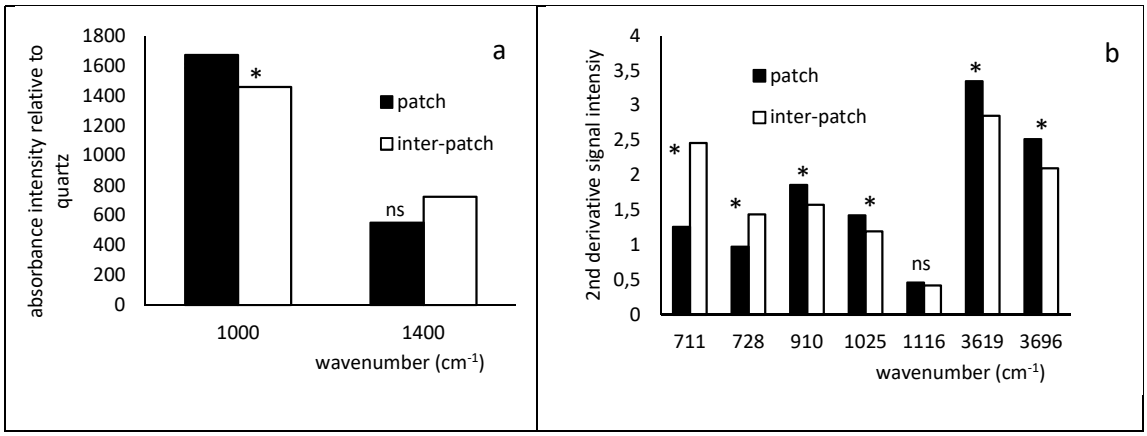

499

500 **Fig. 6** Orihuela soils. a. Intensity of the FTIR spectrum signals respect to quartz. b.

501 Intensity of the second derivative signals for quartz relative to quartz. (*): 0.05>P>0.01;

502 (**): 0.01>P>0.001; (ns): 0.05<P

503

504 Table 1. Geographical and climatic characteristics of the patches under study. The dominant
505 plant species is included in each case

patch	site	altitude (m)	precipitation (mean annual, mm)	utmx	utmy	dominant plant specie
47	Aigües	468	441	731351	4267561	*Ephedra*
48	Aigües	456	441	731388	4267552	*Ephedra*
49	Aigües	443	441	731450	4267575	*R. lycioides*
50	Aigües	442	441	731426	4267561	*R. lycioides*
52	Aigües	443	441	731341	4267486	*Ephedra*
53	Aigües	451	441	731298	4267495	*Ephedra*
54	Aigües	446	441	731368	4267188	*Q. coccifera*
55	Aigües	458	441	731352	4267236	*P. lentiscus*
56	Aigües	462	441	731337	4267248	*Q. coccifera*
57	Aigües	454	441	731371	4267243	*P. lentiscus*
58	Aigües	448	441	731412	4267253	*Q. coccifera*
39	Busot	301	429	726970	4263039	*R. lycioides*
40	Busot	302	429	726966	4263040	*Q. coccifera*
41	Busot	298	429	726917	4263013	*R. lycioides*
42	Busot	295	429	726892	4262967	*Q. coccifera*
43	Busot	283	429	726826	4262872	*R. lycioides*
44	Busot	287	429	726795	4262804	*Ephedra*
45	Busot	277	429	726790	4262826	*P. lentiscus*
46	Busot	277	429	726775	4262752	*P. lentiscus*
24	Campello	68	362	733793	4262717	*Q. coccifera*
25	Campello	89	362	733823	4262899	*P. lentiscus*
26	Campello	106	362	733855	4262900	*R. lycioides*
27	Campello	104	362	733839	4262906	*P. lentiscus*
30	Campello	81	362	733740	4262808	*R. lycioides*
31	Campello	66	362	733756	4262726	*P. lentiscus*
32	Campello	81	362	733730	4262819	*P. lentiscus*
33	Campello	71	362	733746	4262776	*R. lycioides*
34	Campello	64	362	733757	4262770	*Q. coccifera*
1	Orihuela	527	296	678132	4242123	*Q. coccifera*
2	Orihuela	524	296	678142	4242106	*Q. coccifera*
3	Orihuela	525	296	678152	4242141	*Q. coccifera*
4	Orihuela	527	296	678119	4242121	*Q. coccifera*
5	Orihuela	530	296	678083	4242172	*J. oxycedrus*
6	Orihuela	534	296	678114	4242238	*R. lycioides*
7	Orihuela	528	296	678181	4242238	*P. lentiscus*
35	Orihuela	520	296	678215	4242201	*Q. coccifera*
36	Orihuela	544	296	678146	4242299	*J. oxycedrus*
37	Orihuela	522	296	678202	4242218	*P. lentiscus*
38	Orihuela	541	296	678120	4242298	*Q. coccifera*
59	Orihuela	536	296	678147	4242266	*P. lentiscus*
60	Orihuela	525	296	678032	4242165	*J. oxycedrus*

13	Tibi	533	301	709283	4261625	*Q. coccifera*
14	Tibi	525	301	709321	4261624	*Q. coccifera*
15	Tibi	516	301	709323	4261581	*P. lentiscus*
16	Tibi	520	301	709256	4261619	*Q. coccifera*
17	Tibi	516	301	709258	4261607	*R. lycioides*
18	Tibi	523	301	709279	4261626	*J. oxycedrus*
19	Tibi	516	301	709307	4261642	*J. oxycedrus*
20	Tibi	508	301	709347	4261613	*Q. coccifera*
21	Tibi	503	301	709355	4261625	*J. oxycedrus*
22	Tibi	509	301	709318	4261626	*Q. coccifera*
23	Tibi	516	301	709301	4261621	*Q. coccifera*

506

507

Table 2. Soils elemental analysis for patch and inter-patch soils in each location. Total lime measured by calcimetry is also included. nd:not detected

Element	**Aigües**		**Busot**		**Campello**		**Orihuela**		**Tibi**	
(% mol)	patch	inter-patch	patch	inter-patch	patch	inter-patch	patch	inter-patch	patch	inter-patch
Na	0.17±0.05	0.13±0.01	0.21±0.01	0.21±0.02	0.28±0.06	0.25±0.05	0.50±0.07	0.50±0.09	0.31±0.01	0.2±0.2
Mg	1.4±0.1	1.3±0.3	2.6±0.3	2.7±0.5	3.26±0.01	3.26±0.01	6.8±0.4	7.3±0.4	2.5±0.1	2.3±0.4
Al	4.3±0.1	4.0±0.6	9±1	9±2	8.7±0.1	8.6±0.1	19.8±0.8	19.5±0.6	10±2	11±3
Si	10.2±0.6	10±1	22±3	22±3	21±1	22±1	48±2	47±3	27±5	28±6
P	0.2±0.1	0.11±0.01	0.15±0.01	0.122±0.003	0.14±0.01	0.13±0.01	0.33±0.08	0.24±0.02	0.09±0.08	0.09±0.08
S	0.23±0.07	0.14±0.01	0.20±0.05	0.17±0.03	0.25±0.08	0.12±0.09	0.5±0.3	0.27±0.02	0.36±0.04	0.22±0.02
Cl	0.05±0.02	0.02±0.01	0.03±0.01	0.021±0.002	0.05±0.01	0.02±0.02	0.07±0.07	0.02±0.01	0.09±0.02	nd
K	0.85±0.02	0.7±0.2	1.7±0.1	1.6±0.1	1.88±0.01	1.74±0.08	3.6±0.2	3.2±0.2	2.4±0.5	2.3±0.5
Ca	81±1	82±2	62±4	62±5	61±1	61±1	15±1	17±4	54±8	50±10
Ti	0.18±0.01	0.16±0.02	0.3±0.1	0.33±0.04	0.31±0.01	0.30±0.01	0.74±0.03	0.65±0.02	0.5±0.1	0.44±0.07
Cr	nd	nd	0.012±0.004	nd	0.012±0.003	nd	0.013±0.003	0.013±0.003	nd	nd
Mn	0.05±0.02	0.06±0.01	0.061±0.004	0.050±0.003	0.09±0.02	nd	0.11±0.03	0.09±0.01	0.02±0.02	0.02±0.02
Fe	1.31±0.01	1.2±0.2	2.0±0.3	2.0±0.3	2.1±0.08	nd	5.2±0.6	4.53±0.05	3.1±0.8	3.0±0.6
Sr	0.2±0.2	0.06±0.01	0.14±0.02	0.13±0.02	0.18±0.01	0.16±0.01	0.014±0.003	0.011±0.001	0.024±0.004	0.022±0.001
Total lime % weight	87±9	94±8	68±2	67±3	61±1	71±1	5±3	12±2	44±3	60±20